BIOCHEMISTRY
including biophysical chemistry & molecular biology

Article

pubs.acs.org/biochemistry

The Structure and Specificity of the Type III Secretion System Effector NleC Suggest a DNA Mimicry Mechanism of Substrate Recognition

Michelle Marian Turco and Marcelo Carlos Sousa*

Department of Chemistry and Biochemistry, University of Colorado at Boulder, Boulder, Colorado 80309-0596, United States

Supporting Information

ABSTRACT: Many pathogenic bacteria utilize the type III secretion system (T3SS) to translocate effector proteins directly into host cells, facilitating colonization. In enterohemmorhagic *Escherichia coli* (EHEC), a subset of T3SS effectors is essential for suppression of the inflammatory response in hosts, including humans. Identified as a zinc protease that cleaves NF-κB transcription factors, NleC is one such effector. Here, we investigate NleC substrate specificity, showing that four residues around the cleavage site in the DNA-binding loop of the NF-κB subunit RelA strongly influence the cleavage rate. Class I NF-κB subunit p50 is cleaved at a reduced rate consistent with conservation of only three of these four residues. However, peptides containing 10 residues on each side of the scissile bond were not efficiently cleaved by NleC, indicating that elements distal from the cleavage site are also important for substrate recognition. We present the crystal structure of NleC and show that it mimics DNA structurally and electrostatically. Consistent with this model, mutation of phosphate-mimicking residues in NleC reduces the level of RelA cleavage. We propose that global recognition of NF-κB subunits by DNA mimicry combined with a high sequence selectivity for the cleavage site results in exquisite NleC substrate specificity. The structure also shows that despite undetectable similarity of its sequence to those of other Zn^{2+} proteases beyond its conserved HExxH Zn^{2+}-binding motif, NleC is a member of the Zincin protease superfamily, albeit divergent from its structural homologues. In particular, NleC displays a modified Ψ-loop motif that may be important for folding and refolding requirements implicit in T3SS translocation.

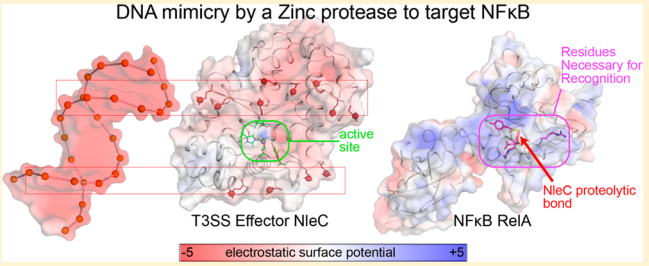

The ability to fight pathogenic γ-proteobacteria with antibiotic drugs led to a drastic decrease in morbidity from bacterial infections in the 20th Century. However, mounting antibiotic resistance makes fighting these deadly microbes more difficult, necessitating new drugs and alternative targets. A tempting target is the pathogenic machinery itself.[1] Many pathogenic bacteria utilize a type III secretion system (T3SS), which consists of secretion machinery that delivers pathogenic proteins, called effectors, into the host cell where they subvert host defenses, thereby facilitating colonization.[2] Distinguished from commensal *Escherichia coli*, enterohemmorhagic *E. coli* (EHEC) belongs to the attaching and effacing (A/E) family of pathogens that are characterized by the effacement of the microvilli of infected epithelial cells upon intimate attachment of the pathogen to the apical membrane.[1,3] The genes for major pathogenic components are located on the locus for enterocyte effacement (LEE), which encodes the T3SS machinery, as well as essential chaperones and effectors.[2,4,5] In addition to these well-characterized components, numerous putative effectors have been identified outside of the LEE in the EHEC O157:H7 Sakai strain.[6]

The major virulence components of the T3SS are the secreted effectors.[2] These proteins are bound by T3SS chaperones upon translation, delivering them to the base of the T3SS needle complex for secretion.[7,8] The effectors must be unfolded to be secreted through the 25 Å T3SS complex needle, which spans the inner and outer membrane of the bacteria, the extracellular space, and connects to a T3SS-inserted pore in the host epithelial cell.[9−11] Once they have been translocated into the host cell, the effectors refold and target various signaling cascades to subvert the host physiology and facilitate infection.[2]

Host cells respond to bacterial infection with an inflammatory response mediated through activation of NF-κB transcription factors, which involves interleukin-8 and TNF-α secretion and results in activation of immunity cells in the underlying basal epithelium.[12−15] NleC (non-LEE effector C) works in concert with other effectors to repress the host inflammation response, facilitating EHEC colonization. NleC is a metalloprotease reported to cleave NF-κB subunits RelA (p65), p50, and c-Rel, thereby depressing downstream transcription events that lead to inflammation.[16−19] Recent publications also implicate NleC in cleaving IκB, preventing phosphorylation of p38, and binding of p300 and CREB-binding proteins.[16,18,20,21]

Received: May 16, 2014
Revised: July 18, 2014
Published: July 18, 2014

   dx.doi.org/10.1021/bi500593e | *Biochemistry* 2014, 53, 5131−5139

With a low level of similarity of its sequence to those of proteases with known structures, NleC was targeted for structural studies to facilitate an understanding of its mechanism. Here we report the structure of NleC from the EHEC Sakai strain refined to 1.9 Å resolution. Through comparison with other zinc proteases, NleC is shown to represent a distinct family within the Zincin fold superfamily. The basis for substrate specificity, defined by activity assays and mutagenesis studies, is also presented. The specificity and structural data are then synthesized into a DNA mimicry hypothesis of substrate recognition.

MATERIALS AND METHODS

Protein Cloning, Expression, and Purification. The gene encoding full-length NleC (residues 1−330) was amplified via polymerase chain reaction (PCR) from EHEC O157:H7 Sakai strain genomic DNA obtained from ATCC. Primers incorporating NdeI and XmaI sites (Table ST1 of the Supporting Information) allowed ligation into a pTYB2 vector (New England Biolabs) that allows the expression of the target gene as a fusion with a self-cleavable intein and a chitin-binding domain at the C-terminus. This plasmid (pMS692) was used to express full-length NleC that, upon self-cleavage of the tag, results in NleC carrying two extra amino acids (PG) at the C-terminus. All fragments of NleC used in this study were amplified via PCR directly from this vector with primers incorporating NdeI and XmaI sites (Table ST1 of the Supporting Information) and cloned into the same vector backbone. NleC mutants were cloned using primer extension mutagenesis (Table ST1 of the Supporting Information).

E. coli BL21(DE3) or Rosetta(DE3) cells (Novagen) were transformed with the desired NleC-expressing plasmid. Cells cultured in LB medium supplemented with ampicillin were grown at 37 °C to an OD_{600} of 0.6. The cells were then incubated on ice for 30 min before expression was induced with 1 mM isopropyl β-D-thiogalactopyranoside (Gold Bio Inc.). After induction, the cells were grown at 20 °C overnight before being harvested by centrifugation. The cells were resuspended in buffer A [25 mM Tris (pH 8.0) and 150 mM NaCl] supplemented with protease inhibitor cocktail [complete ethylenediaminetetraacetic acid-free (Roche)] and either frozen until later use or immediately lysed on ice by sonication. The soluble fraction was separated by centrifugation at 20000*g* for 20 min at 4 °C, added to chitin beads pre-equilibrated with buffer B [25 mM Tris (pH 8.0) and 500 mM NaCl], and incubated for 30 min at 4 °C. The slurry was then packed into a column and washed with at least 10 column volumes of buffer B. The column was then flushed with 2 column volumes of cleavage buffer C [25 mM Tris (pH 8.0), 500 mM NaCl, and 50 mM DL-dithiothreitol (Gold Bio Inc.)] and incubated overnight at 4 °C to allow for cleavage of NleC from the chitin tag. The eluted fractions were concentrated and loaded onto a size-exclusion column (HiLoad 26/60 Superdex 75, Amersham Pharmacia Biotech) pre-equilibrated with buffer A. The NleC-containing fractions were pooled and either concentrated directly or dialyzed into buffer D [20 mM MOPS (pH 7) and 20 mM NaCl], concentrated to a maximal concentration of 30 mg/mL, and stored at 4 °C.

Plasmids encoding human RelA (p65) and p50 were kind gifts from Dr. J. Goodrich (University of Colorado at Boulder). A plasmid encoding RelB was obtained from the Functional Genomics Facility at the University of Colorado at Boulder. The gene fragments encoding RelA (residues 17−291), RelB (residues 124−413), and p50 (residues 39−363) were amplified via PCR and ligated into a modified pHD plasmid obtained from Dr. T. F. Wang (Institute of Biological Chemistry, Academia Sinica, Taipei, Taiwan) following the published procedure.[22] This vector fuses a six-His tag and the yeast small ubiquitin-like modifier (SUMO) at the N-terminus of the target gene. The tag is removed using the Ulp1 SUMO protease (expressed from a plasmid[23] obtained from Dr. C. Lima, Sloan Kettering Institute) that results in a native N-terminus.[23] The gene fragment encoding RelA residues 1−210 was also cloned into a modified pET28 vector that adds an N-terminal His tag and TEV protease site. *E. coli* Rosetta (DE3) cells (Novagen) were transformed with the plasmids and grown in LB medium supplemented with 50 μg/mL kanamycin. Cultures were grown, induced, and harvested, as described above for NleC. After sonication and centrifugation, the soluble fractions of cells were affinity purified on Ni-NTA beads (Qiagen) using buffers containing 1 mM tris(2-carboxyethyl)phosphine to prevent oxidation of cysteines. The purified proteins were concentrated and loaded onto a Superdex 75 column (Amersham Pharmacia Biotech) pre-equilibrated with buffer A. The protein fractions were utilized as eluted or concentrated as necessary. Purified NFATc2 (residues 392−583 with a six-His N-terminal tag) was a kind gift from Dr. J. Goodrich (University of Colorado at Boulder).

NleC Biochemical Assays. The proteolytic activity of NleC on RelA, RelB, p50, and NFATc2 fragments was tested in buffer E [25 mM Tris (pH 8), 150 mM NaCl, and 1 mM TCEP] at various protein concentrations. Cleavage was visualized using sodium dodecyl sulfate−polyacrylamide gel electrophoresis (SDS−PAGE). To test the cleavage efficiency in the presence of DNA, a palindromic 20 bp DNA oligomer (5′-CGGCTGG-AAATTTCCAGCCG-3′) containing the NF-κB consensus sequence GGRRNNYYCC was incubated with RelA at a 1:1 ratio for 1 h prior to the addition of NleC for the activity assay. To define the cleavage sites of RelA, RelB, and p50, the reaction was allowed to proceed overnight and a SDS−PAGE gel overloaded with the products. This gel was electroblotted onto a PVDF Mini Problott membrane (Applied Biosystems) and stained with Coomassie Blue according to the standard procedure. The bands corresponding to the C-terminal pieces of RelA, RelB, or p50 were submitted for N-terminal sequencing by Edman degradation at the University of Texas Medical Branch at Galveston Protein Chemistry Laboratory (Galveston, TX).

Protein Crystallization and Structure Determination. An N-terminal truncation of NleC (residues 17−330) at a concentration of 6 mg/mL yielded crystals after incubation for 5 months with 10% PEG-3350, 50 mM $Mg(CHO_2)_2$, and 0.1 M MES (pH 6.0) in a sitting-drop vapor diffusion experiment (0.2:0.2 protein:precipitant volume ratio). The crystals were transferred to 35% PEG-3350 and 50 mM $Mg(CHO_2)_2$ for 1 min before being flash-frozen in liquid N_2 prior to data collection. A data set to 1.9 Å resolution was collected at the peak, inflection, and remote wavelengths for zinc at the Advanced Light Source at the Lawrence Berkeley National Laboratory (Berkeley, CA). These data were used to determine the structure of NleC using multiwavelength Anomalous dispersion (MAD) methods. All crystallographic calculations were performed using the PHENIX software suite.[24] Using the AutoSol module, one zinc site was identified, corresponding to the active site zinc, and used to calculate MAD phases for density modification. A partial model was built into the resulting electron density map by the AutoBuild module of PHENIX. Manual rebuilding of the model with Coot[25] was alternated with refinement in PHENIX until R_{free} and R_{work} could no longer be improved. The final model

dx.doi.org/10.1021/bi500593e | *Biochemistry* 2014, 53, 5131−5139

Table 1. Data Collection, Phasing, and Refinement Statistics of NleC

	remote	peak	inflection
	Data Collection		
space group		$P2_12_12_1$	
unit cell			
a (Å)		45.21	
b (Å)		67.48	
c (Å)		81.69	
wavelength (Å)	1.2574	1.2831	1.2835
resolution (Å)[a]	50.0−1.9 (1.95−1.9)	50.0−1.9 (1.95−1.9)	50.0−1.9 (1.95−1.9)
R_{sym}[b] (%)	8.1 (48.1)	7.7 (47.0)	7.7 (44.7)
I/σ	13.3 (1.8)	15.8 (1.8)	14.7 (1.5)
completeness (%)	96.4 (97.0)	96.0 (88.2)	96.4 (96.5)
redundancy	2.3 (1.8)	2.4 (1.7)	2.3 (1.8)
	Refinement		
resolution (Å)		34.9−1.9	
no. of reflections		19840	
no. of protein atoms (no H)		2067	
no. of water molecules		186	
R_{work}[c] (%)		18.0	
R_{free}[c] (%)		21.8	
rmsd for bonds (Å)		0.007	
rmsd for angles (deg)		0.993	
mean *B* (Å^2)		28.0	
mean *B* for protein (Å^2)		27.5	
mean *B* for solvent (Å^2)		34.1	
Ramachandran plot (%)			
most favored		97.7	
allowed		2.3	
outliers		0	

[a]Values in parentheses are for the highest-resolution shell. [b]$R_{sym} = \sum_h\sum_i|[I_i(h) - \langle I(h)\rangle]|/\sum_h\sum_I I_i(h)$, where $I_i(h)$ is the *I*th measurement of reflection *h* and $\langle I(h)\rangle$ is the weighted mean of all measurements of *h*. [c]$R_{work} = \sum|F_{obs} - F_{calc}|/\sum F_{obs}$, where F_{obs} is the observed structure factor amplitude and F_{calc} the structure factor calculated from the model. R_{free} is computed in the same manner as R_{work}, but using the test set of reflections.

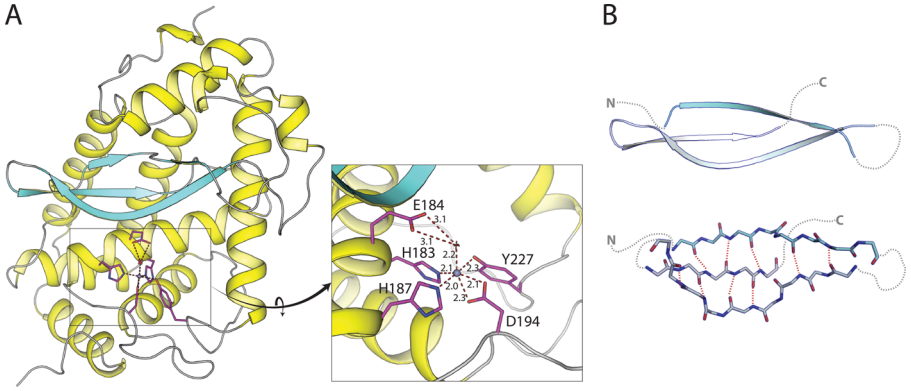

Figure 1. Structure of NleC. (A) Structure of NleC with the active site highlighted. The structure of NleC is shown in standard Zincin coloring as described in Gomis-Ruth et al., with helices colored yellow, strands aqua, and loops gray.[41] The active site residues are shown in magenta stick format. The inset shows a close-up of the active site, including the distances between the zinc and coordinating atoms. (B) Modified Ψ-loop β-sheet motif in NleC. The NleC β-sheet is shown in cartoon and stick format. Red dotted lines represent hydrogen bonds between the strands and illustrate the standard β-sheet interactions between all three strands and the outer two strands after the middle strand exits the sheet.

has NleC residues 22−280 modeled and refined. Data collection, phasing, and refinement statistics are listed in Table 1.

RESULTS

Crystallization and Determination of the Structure of NleC. To gain insight into the mechanism of NleC, we determined the structure of *E. coli* strain Sakai NleC by X-ray crystallography. Whereas the full-length protein was refractory to crystallization, systematic truncations of the N- and C-terminal ends yielded an NleC fragment spanning residues 19−330 that produced well-diffracting crystals. A fluorescence scan revealed that zinc was present in the crystals, consistent with the proposal that NleC was a zinc protease.[16−19] The structure of NleC was determined from one of these crystals using multiwavelength anomalous dispersion (MAD) methods and a three-wavelength data set collected at the Zn^{2+} absorption peak, inflection point, and remote wavelengths (see Materials and Methods for details). The final model, refined to 1.9 Å resolution using the remote

dx.doi.org/10.1021/bi500593e | *Biochemistry* 2014, 53, 5131−5139

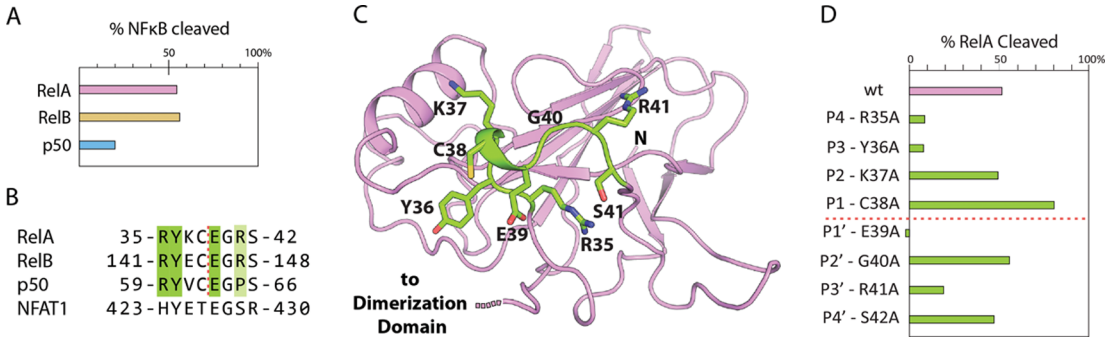

Figure 2. NF-κB proteolysis by NleC. (A) Cleavage of NF-κB subunits by NleC. NF-κB subunits (20 μM), p50, RelA, and RelB, were incubated with 20 nM NleC for 10 min before the reaction was quenched by the addition of SDS−PAGE sample buffer and boiling for 2 min. Results were analyzed by SDS−PAGE. The bands were quantified in ImageJ for visualization in the bar graph. (B) DNA-binding loop in Rel homology domains. Sequence alignment of the residues in the DNA-binding loop of NF-κB subunits RelA, RelB, and p50 as well as transcription factor NFATc2. The scissile bond is shown as a red dotted line. In green are the residues whose mutation to alanine strongly affects NleC cleavage. Light green delineates the arginine that has an intermediate effect on NleC cleavage upon being mutated to alanine, and the proline that is in the same position in p50. The sequence of the NFATc2 DNA-binding loop is shown for reference. (C) DNA-binding loop of RelA containing the scissile bond. Four residues to either side of the scissile bond between cysteine 38 and glutamate 39 are colored green in the DNA-binding domain structure of RelA (PDB entry 2RAM). (D) Cleavage of RelA mutants by NleC. RelA (20 μM), wild type or alanine mutants, was incubated with 20 nM NleC for 10 min before the proteolysis reaction was quenched via addition of SDS−PAGE sample buffer and boiling for 2 min. The results were analyzed by SDS−PAGE and the bands quantified in ImageJ for visualization in bar graph form.

wavelength, contains residues 22−280, a Zn^{2+} ion in the active site, and a Mg^{2+} ion distal from the active site. Data collection, phasing, and refinement statistics are summarized in Table 1.

An NleC fragment (residues 19−287) approximating the crystallographic model is similar to full-length NleC in its ability to cleave the cognate substrate RelA, indicating that the model represents the catalytic core of NleC. Furthermore, Mühlen et al. showed that an NleC fragment similar to the crystallographic model (residues 1−266) was able to abrogate RelA activation in cells as completely as full-length NleC.[16]

NleC Structure. Though NleC has no significant similarity of sequence to any other known protein outside of a conserved zinc-binding motif, HExxH, found in Zincin zinc proteases, the fold of NleC demonstrates it is a member of the Zincin fold superfamily (SCOP FSF d.92.1, PFAM CL0126 Peptidase MA, MEROPS clan MA).[26−28] The structure of NleC consists of eight extended α-helices and three β-strands, cradling the active site zinc (Figure 1A). A hexahydrated magnesium ion is also present in the structure, but it is not coordinated to the protein directly and is not expected to be necessary for function. The zinc-ligating residues are H183, H187, D194, and Y227, while E184 hydrogen bonds a water molecule that is also the sixth Zn^{2+} ligand.

Structural comparisons of NleC with other Zincins reveal that NleC has maintained the basic Zincin fold of a three-helix bundle and mixed β-sheet around the active site. However, the similarity to other known Zincin proteins is limited to topology, with many divergent details. The closest NleC structural relatives, identified utilizing the Dali Server,[29] are aminopeptidase tricorn (Z score = 6.3; rmsd = 3.3 Å) and botulinum toxin (Z score = 5.7; rmsd = 3.3 Å). As illustrated by the relatively high rmsds of the superpositions, the orientation of the conserved basic Zincin fold elements diverges in NleC compared to known Zincins (Figure S1 of the Supporting Information). The presence of a tyrosine coordinating the active site zinc is a rare feature of NleC only seen in the Astacin subfamily of Zincins (MEROPS family M12), which may suggest a close relationship between their folds. However, NleC superimposes on Astacin with an rmsd of 4.3 Å (Z score = 2.4), underscoring the divergence of the structures (Figure S1 of the Supporting Information). NleC also displays a unique feature in its three-stranded β-sheet. Whereas all Zincins contain a Ψ-loop motif within their β-sheets, NleC has a modified Ψ-loop motif zippering the two external strands together upon the exit of the interior strand midway in the β-sheet (Figure 1B). To the best of our knowledge, this modified Ψ-loop has not been described before and a Dali server search with this motif did not identify any similar structures.

NleC Is a Nonpromiscuous Protease Specific for NF-κB Subunits. NleC was previously described as a zinc metalloprotease capable of cleaving NF-κB subunits RelA, p50, and c-Rel.[16−19] Of these NF-κB subunits, only the cleavage site of RelA was defined in the literature, with reports of cleavage between residues 10 and 11 or 38 and 39 near the N-terminus of RelA.[17,19] After purification, we subjected an N-terminal fragment of RelA (residues 1−210) containing the DNA-binding domain to proteolysis by NleC. The cleavage products were isolated by SDS−PAGE and analyzed by Edman amino-terminal sequencing, confirming the cleavage site published by Baruch et al. to be 35-RYKC/EGRS-42. Fragments of RelB (residues 124−413) and p50 (residues 39−363), each containing the DNA-binding domains and dimerization domains, were then analyzed for cleavage by NleC. Digestion of these NF-κB subunits with NleC resulted in cleaved products that were visualized via SDS−PAGE, and the bands corresponding to the cleavage products were subjected to Edman amino-terminal sequencing. RelB was found to be proteolyzed at 141-RYEC/EGRS-148 and p50 at 59-RYVC/EGPS-66. In all three subunits, the scissile bond is contained in a highly conserved DNA-binding loop (Figure 2).

Though the local cleavage site is maintained between the NF-κB transcription factors, further analysis shows the rate of cleavage by NleC differs. Class II NF-κB subunits, RelA and RelB, are cleaved more readily than the class I subunit, p50 (Figure 2A and Figure S2A of the Supporting Information). Because NleC cleaves RelA and RelB with similar efficiency, and most of the published work was conducted with RelA, the further characterization described here was conducted for the RelA DNA-binding and dimerization domains (residues 17−291) only.

To determine which residues in the DNA-binding loop of RelA are important for the recognition by NleC, the residues four positions to either side of the scissile bond in RelA were individually mutated to alanine (Figure 2B−D). These residues

dx.doi.org/10.1021/bi500593e | Biochemistry 2014, 53, 5131−5139

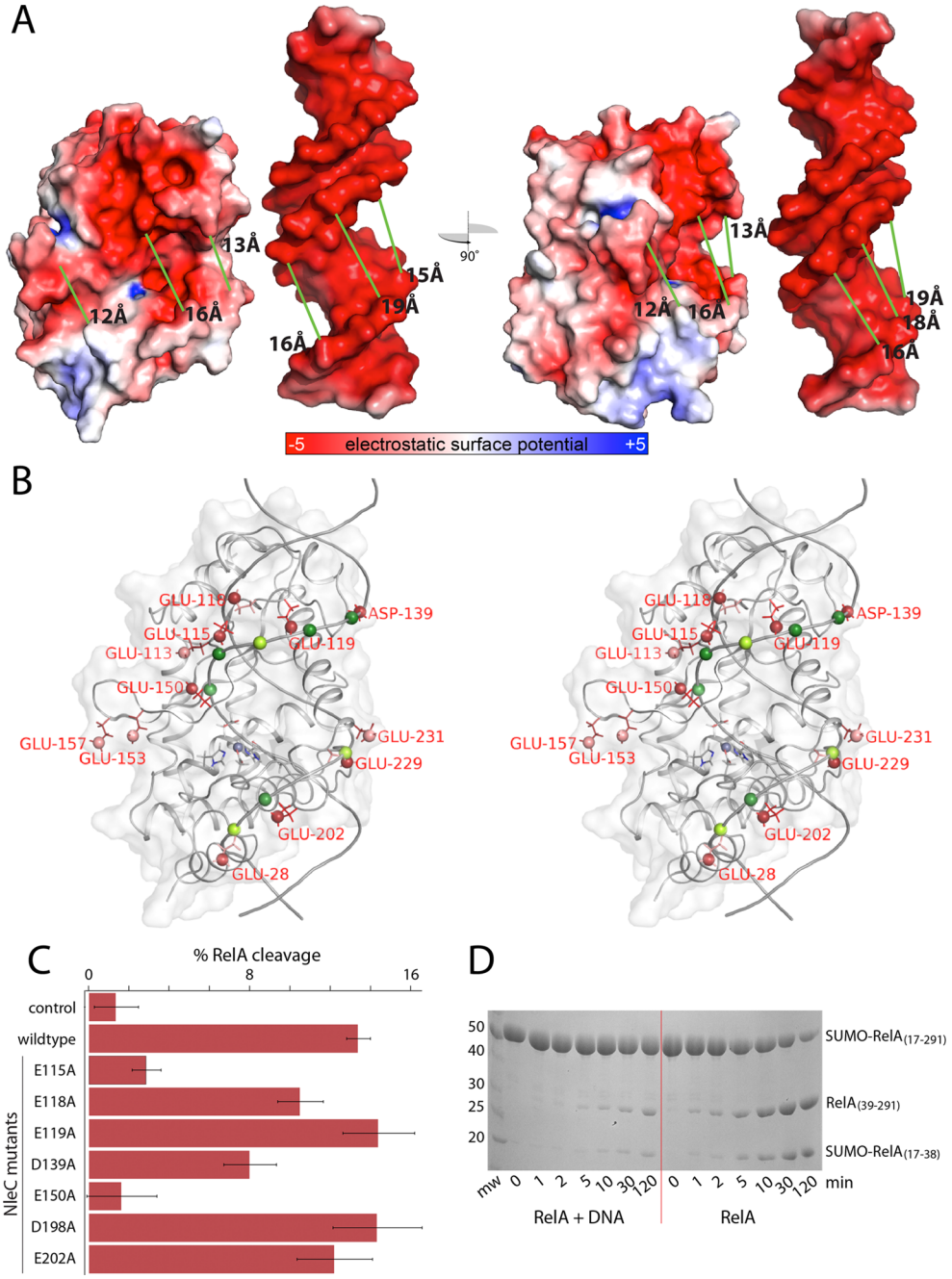

Figure 3. DNA mimicry in NleC. (A) Electrostatic surface potentials of NleC and DNA. Electrostatic surface potentials calculated with APBS[30] are shown mapped to the van der Waals surfaces of NleC and DNA. Green bars illustrate the distances across the major groove of RelA-bound DNA and the active site groove of NleC as measured with Pymol. The right panel is rotated 90° from the left. (B) Superposition of NleC and DNA. Stereoview of the cartoon and semitransparent surface representation of NleC superimposed on a cartoon representation of DNA aligning negatively charged residues in NleC with the phosphate backbone of DNA. Glutamic acid and aspartic acid residues on the active site face of NleC that overlay with DNA phosphates are colored red, and the carboxyl carbon is depicted as a sphere. The carboxyl carbons of other nearby negatively charged residues are depicted as salmon-colored spheres. The phosphates in DNA that are contacted by RelA in the majority of DNA–RelA crystal structures (PDB entries 1RAM, 2RAM, 1LE5, 2I9T, and 3GUT) are colored dark green, with other phosphates that overlay with negatively charged NleC residues colored light green. The superposition was done manually to maximize shape similarity and charge correspondence between NleC and DNA. (C) Alanine scanning mutagenesis of NleC negative charges. RelA (20 μM) was incubated with 20 nM wild-type NleC or 20 nM NleC mutant for 10 min before the reaction was quenched with SDS–PAGE sample buffer and boiling for 2 min. The control reaction mixture contained no NleC. The wild-type NleC reaction was repeated with three biological replicates, which were each tested three times. All NleC mutant reactions are the result of one biological replicate, repeated three times with different dilutions. The results were analyzed by SDS–PAGE and the bands quantified in ImageJ for analysis (Figure S5 of the Supporting Information). The error bars indicate the standard error = standard deviation. (D) Effect of DNA on NleC proteolysis of RelA. After incubation of 20 μM RelA with (left) or without (right) a 1:1 molar ratio of palindromic DNA encoding the RelA-binding site, 20 nM NleC was added and reaction time points were taken. Reactions were quenched via the addition of SDS–PAGE sample buffer and boiling for 5 min and the products analyzed by SDS–PAGE.

dx.doi.org/10.1021/bi500593e | *Biochemistry* 2014, 53, 5131–5139

are named by their relative position from the scissile bond with P4, P3, P2, and P1 being N-terminal to the scissile bond and P1′, P2′, P3′, and P4′ being C-terminal. After purification, the RelA mutants were tested for cleavage by NleC and compared to the wild type. P4 residue R35, P3 residue Y36, and P1′ residue E39 in RelA, when mutated to alanine, significantly reduced the rate of cleavage by NleC, whereas the mutation of R41 had an intermediate effect (Figure 2D and Figure S2B of the Supporting Information). Mutagenesis of P1 residue C38 to alanine increased the cleavage efficiency of NleC, presumably by reducing the size of the P1 residue and alleviating steric hindrance. The steric requirements of this position were further probed by iodoacetamide modification of RelA, which resulted in inhibition of NleC-mediated cleavage ostensibly because of C38 carboxymethylation. Together, these results show that NleC does not specifically recognize C38, but that a smaller residue is preferred at this position. The mutagenesis of P3′ residue R41 had an intermediate effect on cleavage, while the three remaining residues, P2 K37, P2′ G40, and P4′ S42, resulted in a cleavage rate similar to that of wild-type RelA. Conserved among all NF-κB subunits, the three residues most important for cleavage, R35, Y36, and E39, are also clustered together on the structure of the NF-κB subunits (Figure 2C). An additional transcription factor, NFATc2, which contains a Rel homology domain and thus structurally overlays with NF-κB in the DNA-binding domain, was tested for proteolysis by NleC. NFATc2 contains the conserved tyrosine and glutamate that are important for proteolysis by NleC in its DNA-binding loop and, additionally, has an arginine at P4 whose guanidine functional group overlays with P4′ R35 of RelA (Figure S3A of the Supporting Information). Cleavage of NFATc2 would be expected if NleC could recognize all Rel homology domains; however, proteolysis by NleC was not observed (Figure S3B of the Supporting Information).

Though the residues directly surrounding the cleavage site are important for recognition and cleavage by NleC, a small eight-residue peptide harboring these residues is insufficient for proteolysis by NleC. Similarly, a longer 20-residue peptide containing the scissile bond centered between two unrelated proteins could not be cleaved by NleC (Figure S4 of the Supporting Information). Thus, though the RelA DNA-binding loop is essential for cleavage by NleC, distal elements appear to be necessary for efficient cleavage.

DNA Mimicry in NleC. Electrostatic surface potential analysis of NleC, calculated with APBS,[30] reveals that the face containing the active site is extremely negative. The strongly electronegative surface of NleC, combined with the size and shape of the active site cleft, is reminiscent of the major groove of DNA where NF-κB transcription factors bind (Figure 3A). Indeed, a pattern of glutamate and aspartate side chains along the ridges of the active site cleft can be aligned with phosphates in the backbone of DNA that mediate the interaction with RelA in the RelA–DNA structure (Figure 3B).[31] In this superposition, the carboxylate carbons of four negatively charged residues in the upper lip of the NleC active site (E150, E115, E119, and D139) and one on the lower lip (E202, red in Figure 3B) are within ≤2.7 Å of the corresponding phosphates in DNA that are directly contacted by RelA (dark green), although the phosphate mimicked by E202 is hydrogen bonded by RelA in only one (PDB entry 2RAM[31]) of the seven available RelA–DNA structures.[31−35] Other phosphate residues in DNA that are not directly contacted by RelA are colored light green in the superposition, and negatively charged NleC residues E118, E28, and E229 are within 4.3 Å of these, extending the mimicry of the DNA phosphate backbone. Negatively charged E118 in the upper lip is within 6.9 Å of the corresponding phosphate (light green). However, a different rotamer could be modeled to bring the carboxylate within 2.8 Å of the phosphate.

To validate this model, we created alanine mutants of E115, E118, E119, D139, E150, D198, and E202. These mutants were purified in parallel with wild-type NleC and tested for their ability to cleave wild-type RelA. The E150A and E115A mutations had the greatest effect on the ability of NleC to cleave RelA, while an intermediate effect was seen for the D139A and E118A mutations (Figure 3C and Figure S5 of the Supporting Information).

We thus propose that NleC mimics DNA as a strategy for NF-κB recognition. We further suggest that this mimicry mediates the interaction with residues in RelA that are distal from the cleavage site that, as described above, is required for efficient cleavage. Consistent with this proposal, palindromic DNA containing the RelA recognition site inhibited NleC cleavage of RelA (Figure 3D), indicating that NleC and DNA occupy the same binding site on RelA.

DISCUSSION

The observation that NleC was capable of inducing proteasome-independent degradation of NF-κB resulting in abrogation of interleukin-8 secretion in TNF-α-stimulated cells, together with the detection of the Zn^{2+}-binding motif HExxH in the sequence, led to the discovery that NleC is a Zn^{2+} protease.[16−19] The lack of detectable similarity in sequence to any known Zn^{2+} protease beyond the HExxH motif opened the possibility that NleC represented a case of convergent evolution in which a novel fold accommodated the known Zn^{2+} catalytic center. Such a case would be analogous to the classical example of trypsin-like and subtilisin-like families of serine proteases in which the catalytic strategy encoded by the histidine-aspartate-serine triad is accommodated in different folds.[36,37] However, the structure of NleC shows that it retains the topology and structural elements conserved in the Zincin family, albeit with significant divergence from its closest structural homologues, botulinum toxin and tricorn aminopeptidase. These proteins utilize glutamate as the third Zn^{2+}-coordinating residue instead of aspartate and deviate greatly from NleC outside of the Zincin core. The presence of a tyrosine as the final coordinating residue in NleC is rare among Zincins and Zn^{2+}-binding proteins in general.[38,39] Whereas many Zincins contain a tyrosine at this position, it normally serves to hydrogen bond a water molecule that directly coordinates the Zn^{2+}. Direct Zn^{2+} coordination by this tyrosine is only observed in NleC and one other Zincin subfamily, the Astacins (MEROPS family M12).[26,38] However, members of the Astacin Zincin subfamily structurally deviate from NleC outside of the Zn^{2+}-binding site.

The modified Ψ-loop motif in the β-sheet of NleC is very unusual. The canonical Ψ-loop motif is a β-sheet comprised of two consecutive antiparallel strands hydrogen bonded to an additional strand between them. However, the middle strand exits the motif halfway through the β-sheet in NleC. It is thought that Ψ-loops are difficult to fold because one strand has to be inserted between two N-terminal strands. Therefore, it is tempting to speculate that the Ψ-loop modification observed in NleC arose because of evolutionary pressure to select for ease of folding and refolding, which is required for secretion through the narrow needle complex of the T3SS.[9,40]

In contrast to many Zincins, NleC appears to be highly specific. We demonstrated that four residues near the scissile bond of NF-κB subunit RelA, R35 at P4, Y36 at P3, E39 at P1′, and R41 at P3′, are important for cleavage by NleC. In class II NF-κB subunit RelB, these four residues are conserved and RelB was cleaved with an efficiency similar to that of RelA. Analysis of the surface of NleC reveals a large pocket near the active site that overlays with the S1′ pockets of other Zincins that recognize the P1′ substrate position. This P1′ position corresponds to E39 in the conserved RelA DNA-binding loop, and its mutation to alanine ablates proteolysis, consistent with strong P1′ selectivity observed in many Zincins.[41] However, all four residues cited above are determinants for cleavage by NleC, including P3′ residue arginine, whose mutagenesis had an intermediate effect. This is illustrated by the reduced rate of cleavage observed for class I NF-κB subunit p50, which contains a proline in place of arginine at P3′. Similarly, the Rel homology domain of transcription factor NFATc2 is not cleaved by NleC, despite NFATc2 overlaying structurally with NF-κB subunits and having a tyrosine at P3, a glutamate at P1′, and an arginine at P4′, whose guanidinium functional group overlays with the RelA P4 arginine (Figure S3A of the Supporting Information). However, a threonine replaces the cysteine at position P1 from the scissile bond in NFATc2 (Figure 2B). When this residue was mutated to an alanine in RelA, the cleavage efficiency was improved, whereas incubation with iodoacetamide prevented efficient proteolysis. Thus, the larger threonine in NFAT at P1 may partially account for the lack of proteolysis by NleC.

Though residues near the scissile bond in NF-κB are crucial for proteolysis by NleC, cleavage of peptides or fusion proteins containing the RelA DNA-binding loop was not detectable. This suggests that elements distal to the scissile bond are also necessary for recognition and cleavage by NleC. As shown in Figure 3, the active site face of NleC displays a groove and a series of negatively charged residues that can be aligned with the phosphate groups that define the major groove of DNA. This DNA mimicking provides a rationale for the recognition of substrate elements distal from the scissile bond, as residues in RelA that interact with phosphate groups in the DNA−RelA complex may be able to interact with negatively charged residues in NleC. Consistent with this idea, mutation of several of these negatively charged residues to alanine significantly reduced the rate of cleavage of RelA. The residues with the strongest effect on NleC cleavage upon mutagenesis are all located in the upper lip of NleC, above the active site in the standard orientation (E150A, E115A, D139A, and E118A). This observation correlates well with RelA−DNA crystal structures, where RelA makes most of the direct contacts to the DNA backbone with the "upper" strand in the major groove, specifically with the phosphates mimicked by E150, E115, and D139 whose mutation to alanine significantly reduced cleavage efficiency. Only one of the seven crystal structures of the RelA−DNA complex (PDB entry 2RAM)[31−35] shows a significant interaction of RelA with a phosphate in the "lower" DNA strand, and mutation of its mimicking residue (E202) did not have a significant effect on the cleavage of RelA by NleC. Nevertheless, E202 and other phosphate-mimicking negative charges may still be involved in RelA recognition, but their individual mutation was not enough to induce a significant reduction in proteolysis efficiency under the tested conditions. The general pattern of negative charges on the face of NleC may promote electrostatic steering of RelA to the active site of NleC. This is consistent with a recent report showing that negatively charged residues in the NleC structure that are close to the active site are important for efficient proteolysis.[42]

To further test the feasibility of the DNA mimicking hypothesis, we modeled the docking of RelA to NleC by superimposing the phosphate groups in the DNA−RelA complex (PDB entry 2RAM) onto the DNA aligned with NleC (Figure S6 of the Supporting Information). No major clashes between NleC and RelA are observed in the model. Only residues 42 and 43 in RelA partially overlap with residues 195 and 196, which reside in a loop of NleC. However, the main chain atoms in these NleC and RelA residues have temperature factors higher than those of the residues in the rest of the protein main chains (RelA residues 42 and 43, 79.5 $Å^2$; RelA, 46.4 $Å^2$; NleC residues 195 and 196, 34.5 $Å^2$; NleC, 23.3 $Å^2$), suggesting that they may be able to adopt a conformation compatible with this mode of binding. In this simple model, the scissile bond of RelA is located 4.3 Å from the Zn^{2+} ion in the NleC active site, further suggesting that this RelA binding model would be compatible with catalysis.

DNA mimicry has been described for other proteins on the basis of their shape and a pattern of electronegative residues that resemble the disposition of phosphate groups in the major groove of DNA. For example, in eukaryotes, TAF1 mimics DNA to bind the TATA-binding protein, decreasing its transcriptional efficiency.[43−45] Multiple viral proteins that inhibit uracil DNA glycosylase (UDG) have been identified by utilizing similar mechanisms for binding, despite the proteins having no sequence or structural homology. These proteins mimic the phosphate backbone of DNA by providing hydrogen bond acceptors at the same locations and additionally contain a cavity for the UDG hydrophobic residue that is responsible for flipping the uracil residue out of DNA.[45−47] T7 bacteriophage protein Ocr has a broad specificity for type I restriction/modification enzymes, mimicking the overall shape and charge pattern of DNA, and bent to fit in the active sites of these enzymes.[48] In contrast to NleC, these previously described DNA mimics function by stiochiometrically sequestering DNA-binding proteins, whereas NleC possesses enzymatic activity.

In addition to EHEC, NleC genes are found in other enterobacteria, *Vibrio* species, the fish pathogen *Photobacterium damselae*, and the insect pathogen *Arsenophonus nasoniae*. The residues in the active site and in the structural elements around the active site are conserved among all family members (Figure S7 of the Supporting Information), suggesting that all NleC proteins maintain the zinc metalloprotease function. This NleC family is designated in the MEROPS protease database as family M85.[26] With the recent finding that NleC family member Aip56 from *Photobacterium damselae piscicida* also cleaves RelA, it is likely that all NleC proteins share specificity for NF-κB subunits.[49]

Despite the conservation in the catalytic core of NleC family members, the C-termini are divergent starting where the crystallographic model ends. This suggests there may be separate functions for the C-terminal domains of EHEC NleC and other NleC family members. *Photobacterium* Aip56 is an exotoxin with an NleC zinc protease domain at the N-terminus and a C-terminal domain divergent from that of NleC.[49,50] Whereas Aip56 is secreted by an unknown mechanism, its C-terminal domain is required for entry into fish host cells without *Photobacterium* contact, suggesting that a T3SS is not involved. Conversely, NleC is clearly secreted by the T3SS, and it is possible that its C-terminal domain, not present in the structure presented here and not required for cleavage of NF-κB, may be

important for secretion and translocation by the T3SS. It thus appears that NleC family members may represent effectors shared by different secretion systems.

In summary, with NF-κB specificity data and the structure of the NleC catalytic core, we developed a model for their interaction and tested it experimentally. We propose that NleC has evolved a bipartite substrate specificity mechanism recognizing defined amino acids proximal to the cleavage site while mimicking DNA to mediate the interaction with distal elements to efficiently and specifically cleave its NF-κB targets. As a protease, NleC is not required in stoichiometric ratios and is thus more efficient at inhibiting its target than other DNA mimics.

■ ASSOCIATED CONTENT

Supporting Information

Structural and topological comparison of NleC with other Zincins (Figure S1), SDS−PAGE results for NleC cleavage of NF-κB subunits (Figure S2), comparison of NFATc2 to RelA (Figure S3), schematic of the fusion protein containing the NleC cleavage site of RelA (Figure S4), representative SDS−PAGE result for NleC mutant cleavage of RelA (Figure S5), DNA mimicry-motivated model of NleC and RelA interaction (Figure S6), alignment of NleC family members (Figure S7), and plasmids created for this study (Table S1). This material is available free of charge via the Internet at http://pubs.acs.org.

Accession Codes

Coordinate and structure factors for NleC have been deposited in the Protein Data Bank as entry 4Q3J.

■ AUTHOR INFORMATION

Corresponding Author

*Department of Chemistry and Biochemistry, University of Colorado at Boulder, Boulder, CO 80309-0596. E-mail: marcelo.sousa@colorado.edu. Phone: (303) 735-4341.

Author Contributions

M.M.T. and M.C.S. designed the research. M.M.T. performed the research. M.M.T. and M.C.S. analyzed the data and wrote the paper.

Funding

M.M.T. was supported in part by National Institutes of Health Training Grant GM08759. Structural biology research at the University of Colorado at Boulder is supported in part by the William M. Keck Foundation. Part of the work presented in this manuscript was conducted at the Advanced Light Source, which is supported by the Director, Office of Science, Office of Basic Energy Sciences, of the U.S. Department of Energy under Contract DE-AC02−05CH11231.

Notes

The authors declare no competing financial interest.

■ ACKNOWLEDGMENTS

We thank Dr. Amy Dear for initiating the T3SS effector project in the Sousa lab, Dr. J. Goodrich for plasmids encoding RelA and p50 and for purified NFATc2, Dr. T. F. Wang for the SUMO fusion plasmid, and Dr. C. Lima for the Ulp1 expression plasmid.

■ ABBREVIATIONS

NleC, non-LEE-encoded effector C; T3SS, type III secretion system; A/E, attaching and effacing; EHEC, enterohemmorhagic *E. coli*; LEE, locus for enterocyte effacement; MAD, multi-wavelength anomalous dispersion; NF-κB, nuclear factor κ light chain enhancer of activated B cells; IκB, inhibitor of κ-B; Aip56, apoptosis-inducing protein of 56 kDa; CREB, camp response element-binding protein; NFATc2, nuclear factor of activated T cells, cytoplasmic 2; rmsd, root-mean-square deviation; SUMO, small ubiquitin-like modifier; TAF1, transcription initiation factor TFIID subunit 1; TNF-α, tumor necrosis factor α; UDG, uracil-DNA glycosylase; APBS, Adaptive Poisson−Boltzmann Solver; MES, 2-(*N*-morpholino)ethanesulfonic acid; PDB, Protein Data Bank.

■ REFERENCES

(1) Baron, C., and Coombes, B. (2007) Targeting bacterial secretion systems: Benefits of disarmament in the microcosm. *Infect. Disord.: Drug Targets 7*, 19−27.

(2) Wong, A. R. C., Pearson, J. S., Bright, M. D., Munera, D., Robinson, K. S., Lee, S. F., Frankel, G., and Hartland, E. L. (2011) Enteropathogenic and enterohaemorrhagic *Escherichia coli*: Even more subversive elements. *Mol. Microbiol. 80*, 1420−1438.

(3) Donnenberg, M. S., and Kaper, J. B. (1992) Enteropathogenic *Escherichia coli*. *Infect. Immun. 60*, 3953.

(4) McDaniel, T. K., Jarvis, K. G., Donnenberg, M. S., and Kaper, J. B. (1995) A genetic locus of enterocyte effacement conserved among diverse enterobacterial pathogens. *Proc. Natl. Acad. Sci. U.S.A. 92*, 1664−1668.

(5) Frankel, G., Phillips, A. D., Rosenshine, I., Dougan, G., Kaper, J. B., and Knutton, S. (1998) Enteropathogenic and enterohaemorrhagic *Escherichia coli*: More subversive elements. *Mol. Microbiol. 30*, 911−921.

(6) Tobe, T., Beatson, S. A., Taniguchi, H., Abe, H., Bailey, C. M., Fivian, A., Younis, R., Matthews, S., Marches, O., Frankel, G., Hayashi, T., and Pallen, M. J. (2006) An extensive repertoire of type III secretion effectors in *Escherichia coli* O157 and the role of lambdoid phages in their dissemination. *Proc. Natl. Acad. Sci. U.S.A. 103*, 14941−14946.

(7) Akeda, Y., and Galán, J. E. (2005) Chaperone release and unfolding of substrates in type III secretion. *Nature 437*, 911−915.

(8) Thomas, N. A., Ma, I., Prasad, M. E., and Rafuse, C. (2012) Expanded roles for multicargo and class 1B effector chaperones in type III secretion. *J. Bacteriol. 194*, 3767−3773.

(9) Cornelis, G. R. (2006) The type III secretion injectisome. *Nat. Rev. Microbiol. 4*, 811−825.

(10) Ogino, T., Ohno, R., Sekiya, K., Kuwae, A., Matsuzawa, T., Nonaka, T., Fukuda, H., Imajoh-Ohmi, S., and Abe, A. (2006) Assembly of the type III secretion apparatus of enteropathogenic *Escherichia coli*. *J. Bacteriol. 188*, 2801−2811.

(11) Daniell, S. J., Kocsis, E., Morris, E., Knutton, S., Booy, F. P., and Frankel, G. (2003) 3D structure of EspA filaments from enteropathogenic *Escherichia coli*. *Mol. Microbiol. 49*, 301−308.

(12) Hecht, G., and Savkovic, S. D. (1997) Review article: Effector role of epithelia in inflammation—interaction with bacteria. *Aliment. Pharmacol. Ther. 11* (Suppl. 3), 64−69.

(13) MacDonald, T. T., and Pettersson, S. (2000) Bacterial regulation of intestinal immune responses. *Inflammatory Bowel Dis. 6*, 116−122.

(14) Ruchaud-Sparagano, M.-H., Maresca, M., and Kenny, B. (2007) Enteropathogenic *Escherichia coli* (EPEC) inactivate innate immune responses prior to compromising epithelial barrier function. *Cell. Microbiol. 9*, 1909−1921.

(15) Savkovic, S. D., Koutsouris, A., and Hecht, G. (1996) Attachment of a noninvasive enteric pathogen, enteropathogenic *Escherichia coli*, to cultured human intestinal epithelial monolayers induces transmigration of neutrophils. *Infect. Immun. 64*, 4480−4487.

(16) Mühlen, S., Ruchaud-Sparagano, M.-H., and Kenny, B. (2011) Proteasome-independent degradation of canonical NFκB complex components by the NleC protein of pathogenic *Escherichia coli*. *J. Biol. Chem. 286*, 5100−5107.

(17) Yen, H., Ooka, T., Iguchi, A., Hayashi, T., Sugimoto, N., and Tobe, T. (2010) NleC, a Type III Secretion Protease, Compromises NF-κB Activation by Targeting p65/RelA. *PLoS Pathol. 6*, e1001231.

(18) Pearson, J. S., Riedmaier, P., Marches, O., Frankel, G., and Hartland, E. L. (2011) A type III effector protease NleC from

enteropathogenic *Escherichia coli* targets NF-κB for degradation. *Mol. Microbiol. 80*, 219−230.
(19) Baruch, K., Gur-Arie, L., Nadler, C., Koby, S., Yerushalmi, G., Ben-Neriah, Y., Yogev, O., Shaulian, E., Guttman, C., Zarivach, R., and Rosenshine, I. (2010) Metalloprotease type III effectors that specifically cleave JNK and NF-κB. *EMBO J. 30*, 1−11.
(20) Sham, H. P., Shames, S. R., Croxen, M. A., Ma, C., Chan, J. M., Khan, M. A., Wickham, M. E., Deng, W., Finlay, B. B., and Vallance, B. A. (2011) Attaching and effacing bacterial effector NleC suppresses epithelial inflammatory responses by inhibiting NF-κB and p38 mitogen-activated protein kinase activation. *Infect. Immun. 79*, 3552−3562.
(21) Shames, S. R., Bhavsar, A. P., Croxen, M. A., Law, R. J., Mak, S. H. C., Deng, W., Li, Y., Bidshari, R., de Hoog, C. L., Foster, L. J., and Finlay, B. B. (2011) The pathogenic *Escherichia coli* type III secreted protease NleC degrades the host acetyltransferase p300. *Cell. Microbiol. 13*, 1542−1557.
(22) Lee, C. D., Sun, H. C., Hu, S. M., Chiu, C. F., Homhuan, A., Liang, S. M., Leng, C. H., and Wang, T. F. (2008) An improved SUMO fusion protein system for effective production of native proteins. *Protein Sci. 17*, 1241−1248.
(23) Mossessova, E., and Lima, C. D. (2000) Ulp1-SUMO crystal structure and genetic analysis reveal conserved interactions and a regulatory element essential for cell growth in yeast. *Mol. Cell 5*, 865−876.
(24) Adams, P. D., Afonine, P. V., Bunkoczi, G., Chen, V. B., Davis, I. W., Echols, N., Headd, J. J., Hung, L. W., Kapral, G. J., Grosse-Kunstleve, R. W., McCoy, A. J., Moriarty, N. W., Oeffner, R., Read, R. J., Richardson, D. C., Richardson, J. S., Terwilliger, T. C., and Zwart, P. H. (2010) PHENIX: A comprehensive Python-based system for macromolecular structure solution. *Acta Crystallogr. D66*, 213−221.
(25) Emsley, P., and Cowtan, K. (2004) Coot: Model-building tools for molecular graphics. *Acta Crystallogr. D60*, 2126−2132.
(26) Rawlings, N. D., Barrett, A. J., and Bateman, A. (2010) MEROPS: The peptidase database. *Nucleic Acids Res. 38*, D227−D233.
(27) Murzin, A. G., Brenner, S. E., Hubbard, T., and Chothia, C. (1995) SCOP: A structural classification of proteins database for the investigation of sequences and structures. *J. Mol. Biol. 247*, 536−540.
(28) Punta, M., Coggill, P. C., Eberhardt, R. Y., Mistry, J., Tate, J., Boursnell, C., Pang, N., Forslund, K., Ceric, G., Clements, J., Heger, A., Holm, L., Sonnhammer, E. L. L., Eddy, S. R., Bateman, A., and Finn, R. D. (2011) The Pfam protein families database. *Nucleic Acids Res. 40*, D290−D301.
(29) Holm, L., and Rosenström, P. (2010) Dali server: Conservation mapping in 3D. *Nucleic Acids Res. 38*, W545−W549.
(30) Baker, N. A., Sept, D., Joseph, S., Holst, M. J., and McCammon, J. A. (2001) Electrostatics of nanosystems: Application to microtubules and the ribosome. *Proc. Natl. Acad. Sci. U.S.A. 98*, 10037−10041.
(31) Chen, Y. Q., Ghosh, S., and Ghosh, G. (1998) A novel DNA recognition mode by the NF-κB p65 homodimer. *Nat. Struct. Biol. 5*, 67−73.
(32) Berkowitz, B., Huang, D. B., Chen-Park, F. E., Sigler, P. B., and Ghosh, G. (2002) The X-ray crystal structure of the NF-κB p50.p65 heterodimer bound to the interferon β κB site. *J. Biol. Chem. 277*, 24694−24700.
(33) Chen-Park, F. E., Huang, D. B., Noro, B., Thanos, D., and Ghosh, G. (2002) The κB DNA sequence from the HIV long terminal repeat functions as an allosteric regulator of HIV transcription. *J. Biol. Chem. 277*, 24701−24708.
(34) Escalante, C. R., Shen, L., Thanos, D., and Aggarwal, A. K. (2002) Structure of NF-κB p50/p65 heterodimer bound to the PRDII DNA element from the interferon-β promoter. *Structure 10*, 383−391.
(35) Stroud, J. C., Oltman, A., Han, A., Bates, D. L., and Chen, L. (2009) Structural basis of HIV-1 activation by NF-κB: A higher-order complex of p50:RelA bound to the HIV-1 LTR. *J. Mol. Biol. 393*, 98−112.
(36) Doolittle, R. F. (1994) Convergent evolution: The need to be explicit. *Trends Biochem. Sci. 19*, 15−18.
(37) Kester, W. R., and Matthews, B. W. (1977) Comparison of the structures of carboxypeptidase A and thermolysin. *J. Biol. Chem. 252*, 7704−7710.
(38) Gomis-Ruth, F. X. (2009) Catalytic Domain Architecture of Metzincin Metalloproteases. *J. Biol. Chem. 284*, 15353−15357.
(39) Patel, K., Kumar, A., and Durani, S. (2007) Analysis of the structural consensus of the zinc coordination centers of metalloprotein structures. *Biochim. Biophys. Acta 1774*, 1247−1253.
(40) Galán, J. E., and Wolf-Watz, H. (2006) Protein delivery into eukaryotic cells by type III secretion machines. *Nature 444*, 567−573.
(41) Gomis-Rüth, F. X., Botelho, T. O., and Bode, W. (2012) A standard orientation for metallopeptidases. *Biochim. Biophys. Acta 1824*, 157−163.
(42) Li, W., Liu, Y., Sheng, X., Yin, P., Hu, F., Liu, Y., Chen, C., Li, Q., Yan, C., and Wang, J. (2014) Structure and mechanism of a type III secretion protease, NleC. *Acta Crystallogr. D70*, 40−47.
(43) Liu, D., Ishima, R., Tong, K. I., Bagby, S., Kokubo, T., Muhandiram, D. R., Kay, L. E., Nakatani, Y., and Ikura, M. (1998) Solution structure of a TBP-TAF(II)230 complex: Protein mimicry of the minor groove surface of the TATA box unwound by TBP. *Cell 94*, 573−583.
(44) Anandapadamanaban, M., Andresen, C., Helander, S., Ohyama, Y., Siponen, M. I., Lundström, P., Kokubo, T., Ikura, M., Moche, M., and Sunnerhagen, M. (2013) High-resolution structure of TBP with TAF1 reveals anchoring patterns in transcriptional regulation. *Nat. Struct. Mol. Biol. 20*, 1008−1014.
(45) Putnam, C. D., and Tainer, J. A. (2005) Protein mimicry of DNA and pathway regulation. *DNA Repair 4*, 1410−1420.
(46) Cole, A. R., Ofer, S., Ryzhenkova, K., Baltulionis, G., Hornyak, P., and Savva, R. (2013) Architecturally diverse proteins converge on an analogous mechanism to inactivate uracil-DNA glycosylase. *Nucleic Acids Res. 41*, 8760−8775.
(47) Putnam, C. D., Shroyer, M. J., Lundquist, A. J., Mol, C. D., Arvai, A. S., Mosbaugh, D. W., and Tainer, J. A. (1999) Protein mimicry of DNA from crystal structures of the uracil-DNA glycosylase inhibitor protein and its complex with *Escherichia coli* uracil-DNA glycosylase. *J. Mol. Biol. 287*, 331−346.
(48) Walkinshaw, M. D., Taylor, P., Sturrock, S. S., Atanasiu, C., Berge, T., Henderson, R. M., Edwardson, J. M., and Dryden, D. T. F. (2002) Structure of Ocr from bacteriophage T7, a protein that mimics B-form DNA. *Mol. Cell 9*, 187−194.
(49) Silva, D. S., Pereira, L. M. G., Moreira, A. R., Ferreira-da-Silva, F., Brito, R. M., Faria, T. Q., Zornetta, I., Montecucco, C., Oliveira, P., Azevedo, J. E., Pereira, P. J. B., Macedo-Ribeiro, S., Do Vale, A., and Dos Santos, N. M. S. (2013) The Apoptogenic Toxin AIP56 Is a Metalloprotease A-B Toxin that Cleaves NF-κb P65. *PLoS Pathol. 9*, e1003128.
(50) Wilkes, T. E., Darby, A. C., Choi, J. H., Colbourne, J. K., Werren, J. H., and Hurst, G. D. D. (2010) The draft genome sequence of *Arsenophonus nasoniae*, son-killer bacterium of *Nasonia vitripennis*, reveals genes associated with virulence and symbiosis. *Insect Mol. Biol. 19*, 59−73.